Research Paper © 2012 IJFANS. All Rights Reserved

Preparation and Characterization of low-cost activated carbon prepared from Skin of *Allium sativum* and *Zingiber officinale.*

J.JOSE HEPZIN ALIS[1] and Dr.M.JAYA RAJAN[2]

1.Research scholar(19213012032005), Department of chemistry & Research centre, Annaivelankanni, college, Tholayavattam.Affiliated to Manonmaniamsundaranar university, Abishekapatti, Tirunelveli-627012, Tamil Nadu, India.
2.Associate Professor, Department of Chemistry researchcentre, AnnaiVelankanni college, Tholayaattam, India.
Corresponding Author:aliceantonyezhil@gmail.com
Mobile Noumber:8526351757

Abstract:

Activated carbon was prepared from skin of *Allium sativum* and *Zingiber officinale*. Pottasium hydroxide is widely used as an activating agent for preparation of activated carbon. The microscopic and spectroscopic methods such as BET, XRD, TGA/DTA, FT-IR, and SEM with EDAX, aspect of their power to directly view the micro-structure of activated carbons have huge potential for utilize in the inquiry and characterization of AC. Using BET method to determine the surface area, pore volume, and pore size of prepared activated carbon adsorbent before activation and after chemical KOH activation. Results showed that, surface area, pore volume, and pore size increases due to KOH activation. The X-ray patterns of AC prepared from skin of *Allium sativum* and *Zingiber officinale* proved the amorphous structure of activated carbon, and had observable lump in the range 20℃- 30℃. That indicates, the state of disorder of an activated carbon.TG/DTA suggested that, the ASACis stable upto 450℃ and completely degraded at 664℃. Similarly ZSAC is stable upto 513℃ and completely degraded at 706℃. FT-IR analysis of ASAC and ZSAC revealed the presence of OH stretching vibration, asymmetric and symmetric C-H stretching vibration, C=C stretching vibration. In SEM_EDX analysis it can be surmised that the, prepared ASAC and ZSAC existing enough morphology for Cu(II) ion and Cr(VI) ion adsorption.

Keywords:

Cu(II) ions, Cr(VI) ions, Skin of *Allium sativum* and *Zingiber officinale* activated carbon, Characterization.

1 Introduction:

Activated carbon is a form of carbon that has small, low size volume of pores that increase the surface area and increases the adsorption process. It has high degree of micro porosity. The utmost very significant parameter that is set into consideration is to probe its characterization is microporosity. The microscopic and spectroscopic methods such as XRD, FT-IR, TGA/DTA and SEM with EDAX, aspect of their power to directly view the micro- structure of activated carbons have huge potentiality for utilize in the inquiry and characterization of low cost activated carbon. (Manocha et al, 2010). Activated carbon is an amorphous form of carbon. The have high pore size and surface area. Its porous structure allows it to specially adsorb other non- polar compounds and organic materials from gas or liquid streams (Lumadede, 2002). Because of its high adsorption capacity, utmost utilised adsorbent is activated carbon and most technically important adsorbents.(Song et al, 2006) The zeta potential measurements gives idea to understanding the surface chemistry of an adsorbent. that indicate the net charge of an adsorbent when it comes in contact with aqueous solution. (Shahanaz Parvin and Biplob kumar Biswas, 2021).

2. Materials and Methods:

2.1 **Preparation of activated carbon adsorbent** The activated carbon adsorbents used for the experiments are allium sativum skin and zingiber officinale skin.

Fig 1 Schematic diagram for preparation method of activated carbon.

The peels of *Allium sativum* and *Zingiber officinale* were collected at Thuckalay from cottage industry, hotel waste, and kitchen waste from Thuckalay, Kanyakumari, Tamilnadu, India and were washed to remove dust and soluble impurities and dried in sunlight for 7 days. About 500g of the sample was weighed and then the converted into charcoal in a muffle furnace at 400℃ for 1 hour before being activated (Oliveira et al., 2018) and the sample was obtained were soaked in a 1:4 KOH solution for 12 hours and followed by weighing the sample in order to know activation in a muffle furnace at different temperature 250℃, 300℃, 350℃, 400℃, 450℃ and 500℃ for 2 hours. The carbonized material was washed with distilled water to remove the free alkalis and dried at 100 ±5℃ 2hrs and weighed to calculate the yield. (Hariprasad Petal, 2016).

In this study, Pottasium hydroxide is widely used as an activating agent for preparation of activated carbon. It is evident that KOH activation produces activated carbon with a greater specific surface area and good pore development but the

resulting yield is typically low, due to the development of pores, which accelerates the carbon loss as a result of the intercalation of metallic potassium ions into the carbon network. (Prahas et al, 2007).
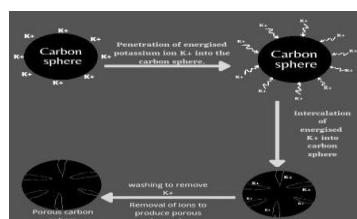
Fig 2 Pore development of activated carbon during activation process.

The activated carbon yield is lower at increase activation temperatures due to KOH may catalyze the oxidation reaction (Fierro et al, 2007).

2.2 Characterization study of activated carbon
Low cost activated carbon adsorbent's surface area was analysed using BEL Sorp max from microtrac, BEL Corp, Japan with nitrogen adsorption. The cell hang the activated carbon sample were weighed before degasification. The activated carbon sample was warmed at 10°C/ min to 110°C, held for 15 min and then warmed to 200°C at 10°C/ min and hold for 2hrs.

X- ray diffraction studies had showed that the structure of activated carbon was same to that of amorphous form of carbon. (XRD BRUKER D2 PHASER) .

The thermogravimetric of the activated carbon adsorbent materials, before adsorption of metals, were recorded in an SIINT 63000, Japan employing the method 0°C-1000°C under air atmosphere.

The FT-R spectra of the activated carbon adsorbent materials before and after adsorption of metals were recorded KBr pellets by using a SHIMADZU FTIR8400s. (Frequency range: $400\text{-}4000cm^{-i}$).

The scanning electron microscope (SEM) photographs of the activated carbon adsorbent materials before and after adsorption of metal were obtained using a JEOL JSM 6390 Japan. A SEM is used to study the outer surface, microporosity and pore size of activated carbon.

3 Results and Discussions

3.1 BET Analyzis

The pore size, volume of pore and surface area of selected AC adsorbents *Alivam sativum* (AS) and

Zingiber officinale (ZS) both before activation and after activation using KOH were analysed with

nitrogen adsorption and desorption environment. The analysis of pore size, pore volume and surface

area was carried out on the basis of volume of gas adsorbed at different relative pressures. Adsorption

desorption iosotherm of the samples AS and ZS before and after activation correspond to type IV

isotherm (khalfaoui *et al.,* 2003) are shown in Figure 3.. The area under loops increased with

increasing pressure up to saturation thereby increasing the surface area, the pore size, and the pore volume. The results was tabulated in Table 1.

Table 1   Volume of monolayer adsorption capacity (V_m) specific Surface area, Pore Volume, Pore Size of AC Adsorbent

Activated carbon	V_m cm^{3}g	Specific surface area m²/g	Pore volume cm³/g	Pore size nm
AS (before activation)	193	840	0.01766	7.0203
AS (after activation) (or) ASAC	526	2289	0.0533	15.560
ZS (before activation)	135	588	0.0290	6.7650
ZS (after activation) (or) ZSAC	357	1557	0.04969	16.177
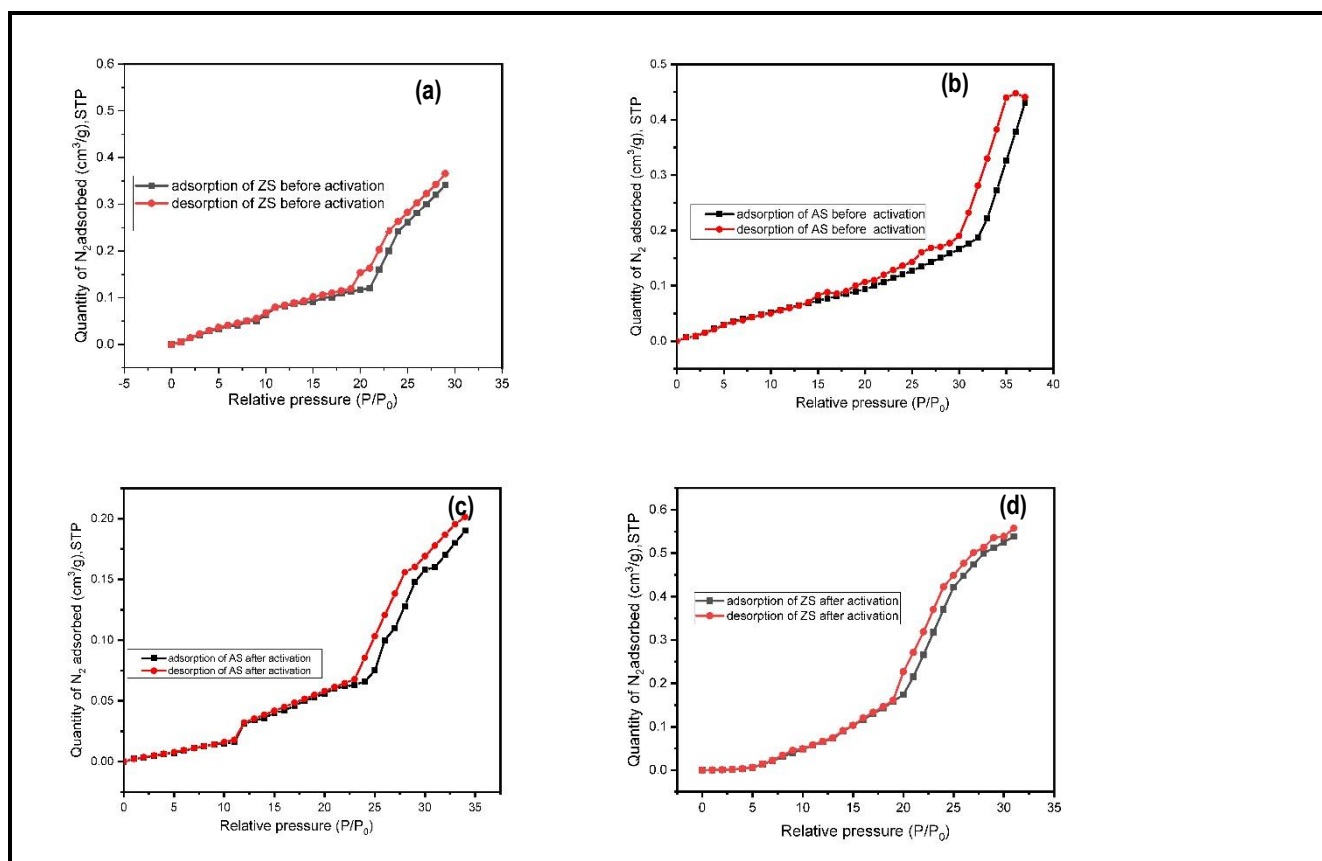
Fig. 3   BET plot for (a) AS before activation, (b) AS after activation, (c) ZS before activation and (d) ZS after activation

In the present analysis, surface area were ~840 m^2/g, ~ 588 m^2/g, pore volume 0.0177 cm^3/g, 0.0290 cm^3/g, pore size 7.0203 nm, 6.7650 respectively for skin of *Allium sativum* (AS) and *Zingiber officinale* (ZS) for before activation.

Similarly surface area ~ 2289 m^2/g, ~ 1557 m^2/g, pore size 15.560 nm, 16.177 nm respectively for skin of AS and ZS for after activation with KOH.

During KOH activation, pore size, pore volume, specific surface area increased. Higher porosity percentage tends to increase the adsorption sites of the adsorbents, hence improves the adsorption capacity of such adsorbents (Vunain *et al.,* 2017).

3.2 XRD Analysis

X-ray diffraction spectroscopy for *Allivum sativum* skin activated carbon (ASAC) was shown in Fig 4.(a). At 23.16° and 45.05°. Bragg's law is fulfilled for the (002) and (001) planes, producing a diffraction peak. The values are listed in (Table 2(a)).
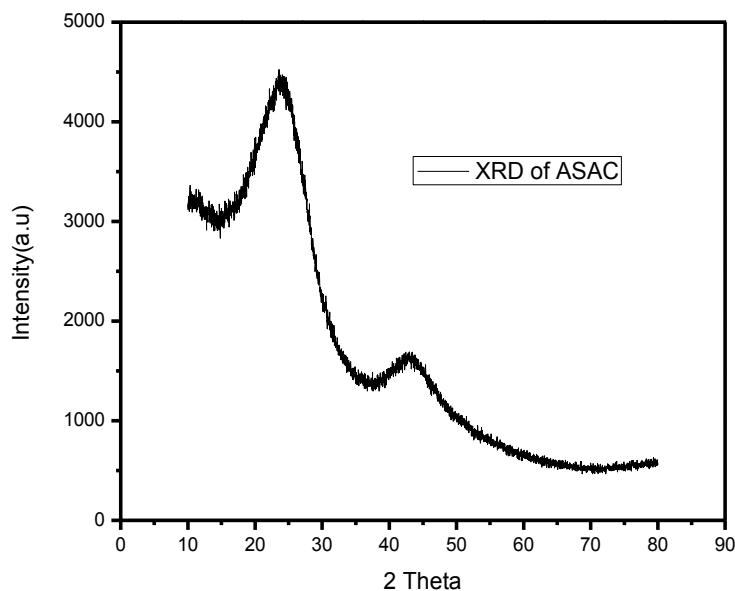
Fig. 4(a) XRD spectrum of ASAC

Table 2(a) D spacing for planes of ASAC

2θ	Diffraction peaks for AC	D spacing A°
23.16°	002	3.8374
45.05°	001	2.0108

X-ray diffraction spectroscopy for *Zingiber Officinale* skin activated carbon (ZSAC) was shown in Fig 4(b). At 26.01° and 44.36°. Bragg's law fulfilled for the (002) and (001) planes, producing a diffraction peak. The values are listed in Table 2(b)).
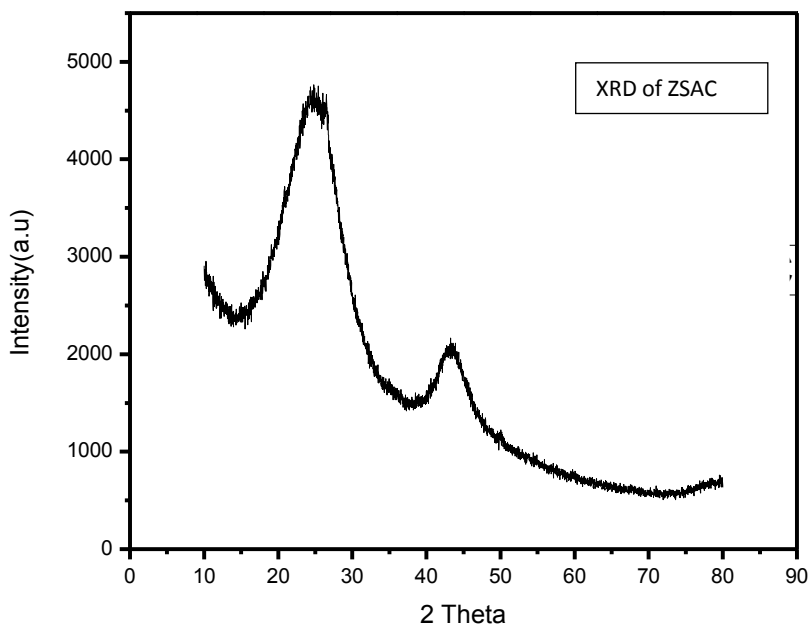
Fig 4(b) XRD spectrum of ZSAC

Table 2 (b) D spacing for planes of ZSAC

2θ	Diffraction peaks for AC	D spacing A°
26.01°	002	3.4230
44.36°	001	2.0404

XRD studies showed that ASAC and ZSAC were amorphous in nature. XRD pattern also indicated that, an observable broad peak in the range of 20-30°, indicates the state of disorder of an AC (Bohli et al., 2015).

3.3 TGA/DTA Analysis

TGA/DTA Studies were analysed to determine the decomposition temperature and the stability. It is the method in which the changes in physical as well as chemical properties of an activated carbon were studied with respect to temperature.

Figure 5 (a) illustrates the TGA/DTA measurement of *Allium sativum* activated carbon (ASAC). The data showed two exothermic peaks with a maximum at 506°C and 637°C resulting in a loss of total weight. There were three curves appeared from TGA spectrum. The first type of weight loss occurred at temperatures between 30°C to 98.85°C due to the emission of water molecules and moisture from the activated carbon.

The second type of weight loss obtained in the temperature range of 98.85°C to 450°C which could be due to the evaporation of inorganic element from activated carbon (Vunain *et al.,* 2017).

The high percentage of weight loss obtained in the range of 450°C to 664°C. The corresponding weight loss percentage were presented in the Table 3. The complete removal of moisture, water and inorganic residue to gives the pure activated carbon and also the present investigation confirmed that ASAC were stable upto 450°C and completely degraded at 664°C (Yagsi, 2004).
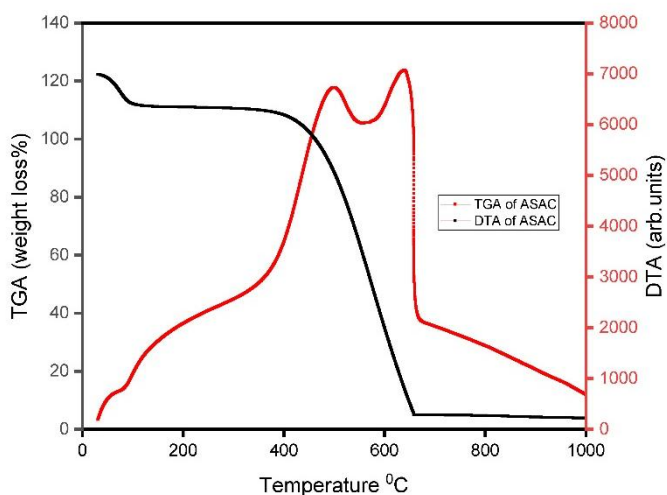
Fig. 5(a) TGA/DTA curve for ASAC

Similarly *Zingiber officinale* activated carbon (ZSAC) are shown in Figure 5 (b). The data showed an exothermic peak at 675°C resulting in a loss of total weight. Tere were three curves appeared from TGA spectrum. The first type of weight loss occurred at temperature between 34.18°C to 102.76°C. The second type of weight loss obtained in the temperature range of

102.76°C to 513°C. The high percentage of weight loss obtained in the range of 513°C to 706°C. The corresponding weight loss percentage were tabulated in the Table 3. These studies confirmed that ZSAC were stable up to 513°C and completely degraded at 706°C.
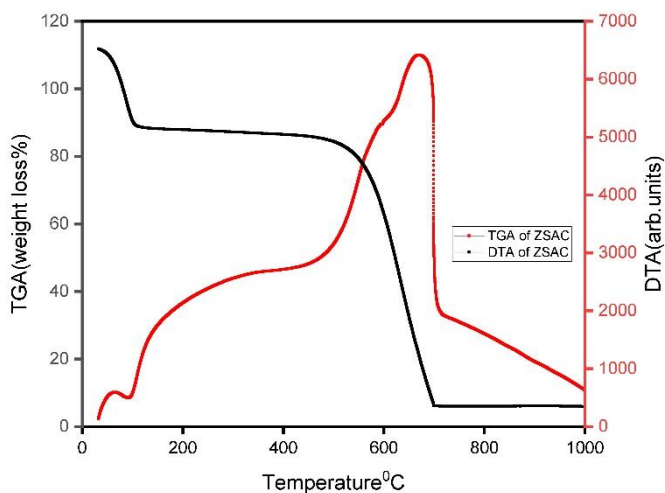
Fig. 5(b) TGA/DTA curve for ZSAC

Table 3 Weight loss percentage of AC prepared from ASAC and ZSAC

Sl. No.	Activated Carbon	Temparture °C		Total weight loss (%)
		Initial	Final	
1	ASAC	30	98.85	11.24
		98.85	450	8.95
		450	664	97.61
2	ZSAC	34.18	102.76	22.66
		102.76	513	5.39
		513	706	78.27

3.4 FT-IR studies of the activated carbon

The FT-IR spectroscopic method was used to analyze the which functional groups were present in the *Allivum sativum* activated carbon (ASAC) and *Zingiber officinale* activated carbon (ZSAC) adsorbents which was shown in Figure 6 (a) & (b) and the values are tabulated in Table 4. (a) & (b). The FT-IR analysis is also quite popular for analysing material on the surfaces of AC (Fan *et al.,* 2012).

The FT-IR spectral studies of ASAC and ZSAC adsorbents were presents the following vibrational peaks, such as OH stretching vibration, symmetric and asymmetric C-H stretching vibration, C = C stretching vibration, and C = O stretching vibrations are tabulated in the Table 4(a) and (b). The presence of OH and C = O as a surface functional groups is due to chemical KOH activation (Sahira and Bhadra, 2013).
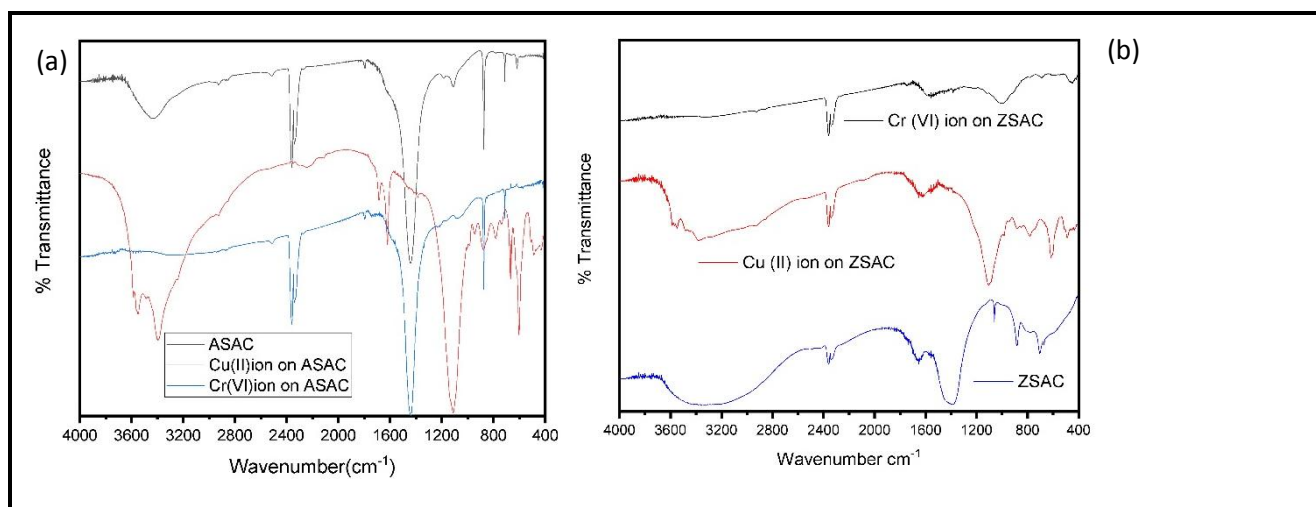
Fig. 6 (a) FT-IR spectrum of ASAC, Cu(II) ion and Cr(VI) ion on ASAC
(b) FT-IR spectrum of ASAC, Cu(II) ion and Cr(VI) ion on ZSAC

The FT-IR spectrum of activated carbon shows an intense and broad peak at 3429.55 cm^{-1} for ASAC and 3684.11 cm^{-1} for ZSAC indicates the presence of hydroxyl group, H-bonded OH stretching vibration of AC sample. (Abdel- Nasser and Hendawy, 2006). These following peaks are presence in the FT-IR spectra of ASAC and ZSAC adsorbents between the frequency in the range of 1462.12 cm^{-1}, 1112.45 cm^{-1} and 871.96 cm^{-1} for ASAC and 1399.39 cm^{-1}, 1049.47 cm^{-1} and 883.34 cm^{-1} for ZSAC indicates the basic hydroxyl group (-OH) present in the surface of the AC sample are hydroxylated (Chen *et al.,* 2008).

The two strong peaks present in the close range between 2928.86 cm^{-1} and 2930 cm^{-1} and 2500 cm^{-1} corresponded to the asymmetric and symmetric stretching C-H stretching vibration of ASAC and ZSAC. The observed peak at 2524.21 cm^{-1} for ASAC and 2349.77 cm^{-1} for ZSAC represent the presence of a C-C single bond (Asep *et al.,* 2019). The peak at

1797 cm^{-1} for ASAC and 1668.99 cm^{-1} for ZSAC is due to the presence of carbonyl compound (Tongpoothorn *et al.,* 2019; Asep *et al.,* 2019). The peak at 871.96 cm^{-1}, for ASAC and 883.34cm^{-1} for ZSAC was due to C-H bending of AC. (Eren and Afsin, 2008).

Table 4 (a)   Interpretation of FTIR band positions of ASAC before binding metal ions after binding metal ions of Cu(II) ion and Cr(VI) ion in wave number (cm^{-1})

Assignment (cm^{-1})	Before binding metal ions	After binding metal ions	
		Cu(II) ion	Cr(VI) ion
O-H stretching	3429.55 (broadband)	3573.19 to 3402.46	Destabilised
C-H stretching	2928.86 to 2930	2229.55	Destabilised
C-C stretching	2524.21	1674.69	2531.60
C=C stretching	2352.67	1632.83	2360.05
Carbonyl Compound	1797	1407.11	1756.77
O-H bending	1462.12	1132.97	1454.72
O-H association (cell work)	1112.45	879.34	1070.59
C-H bending	871.96	591.24	865.39

Table 4 (b)   Interpretation of FTIR band positions of ZSAC before binding metal ions after binding metal ions of Cu(II) ion and Cr(VI) ion in wave number (cm^{-1})

Assignment (cm^{-1})	Before binding metal ions	After binding metal ions	
		Cu(II) ion	Cr(VI) ion
O-H stretching	3684.11	3512.56 to 3361.42	Destabilised
C-H stretching	2500	2923	2925.81
C=C stretching	2349.77	2349.77	2349.77
Carbonyl Compound	1668.99	1662.18	1579.12
O-H bending	1399.39	1110.74	1014.07

| O-H association (cell work) | 1049.47 | 842.51 | 794.86 |
| C-H bending | 883.34 | 759.46 | 698.18 |

The present studies revealed that after adsorption of Cu(II) ion on AC, the absorption bands are shifted from higher to lower frequency region (Anah and Astrini, 2010). This is because of the involvement of the functional groups that are present in the binding of AC with metal ion (Abuzer and Husegin, 2011; Azouaou *et al.,* 2010).

3.5 Morphological Study
3.5.1 SEM Analysis

To investigate the morphology of activated carbon and loaded metal ions, SEM analysis was performed. Scanning electron microscopy (SEM) methodology is utilized to analyze the microstructure of the *Allium sativum* activated carbon (ASAC), and *Zingiber officinale* activated carbon (ZSAC) before and after adsorption of metal ions. The SEM image illustrates the average particle size as well as surface topography of the activated carbon adsorbent (Ismail *et al.,* 2009).

SEM images of the ASAC Cu (II) ion loaded ASAC, and Cr (VI) ion loaded ASAC were shown in Figure 7.
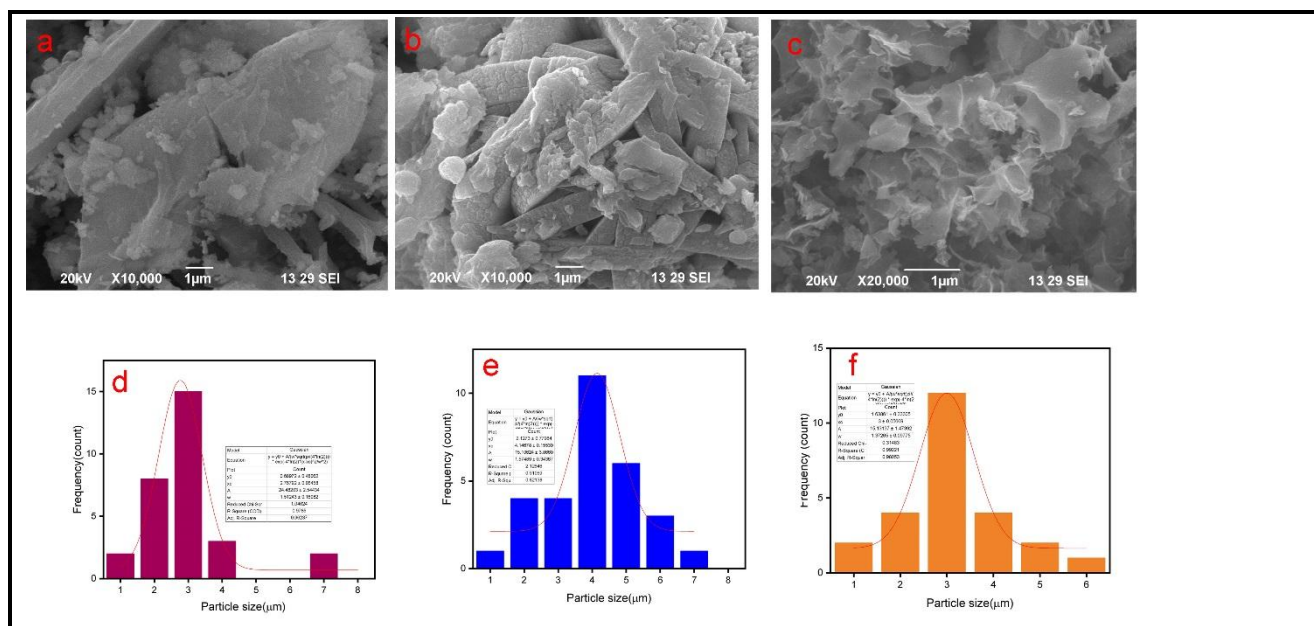
Fig. 7   **Scanning electron micrographs of (a) ASAC, (b) Cu(II) ion on ASAC and (c) Cr(VI) ion on ASAC, Particle size distribution gram graph of (d) ASAC, (e) Cu(II) ion on ASAC and (f) Cr(VI) ion on ASAC**

Similarly SEM images of ZSAC, Cu (II) ion loaded ZSAC, and Cu (VI) ion loaded ZSAC were shown in Figure 8.
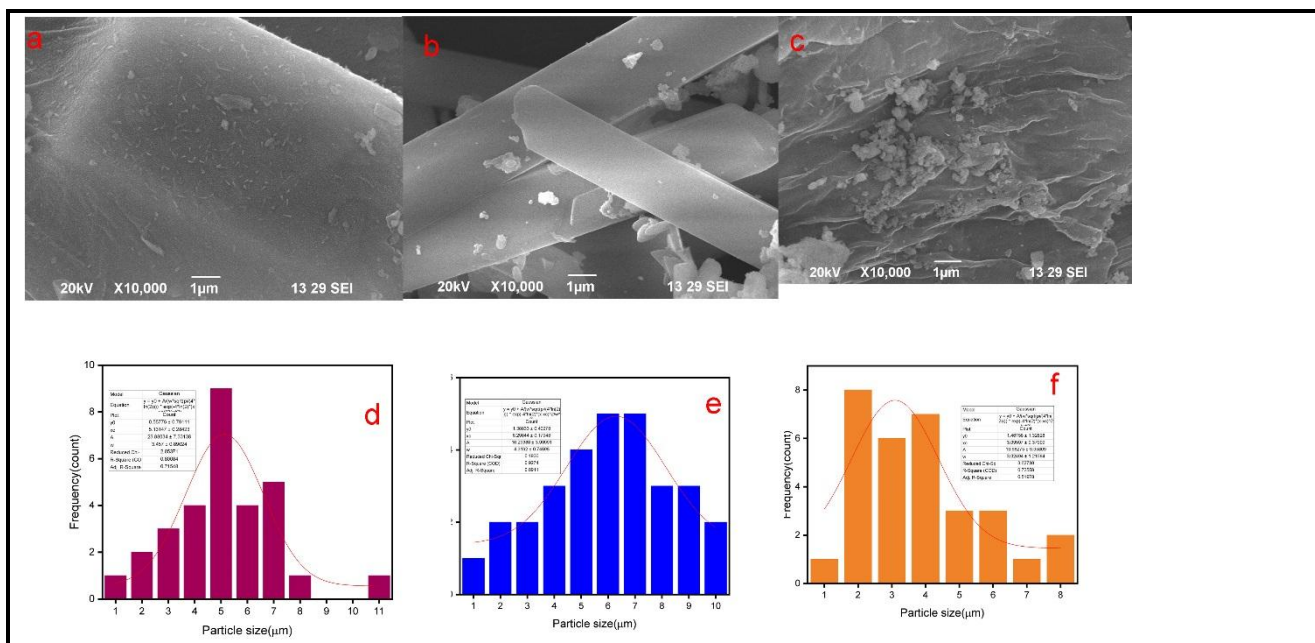
Fig. 8   **Scanning electron micrographs of (a) ZSAC, (b) Cu(II) ion on ZSAC and (c) Cr(VI) ion on ZSAC, Particle size distribution gram graph of (d) ZSAC, (e) Cu(II) ion on ZSAC and (f) Cr(VI) ion on ZSAC**

The Bright spots / pores found on the surface of activated carbon suggested that, during adsorption process contact area increases and as well as encourage pore diffusion (Parmar *et al.,* 2006), which is the main factors that increase the adsorption capacity (Ismail *et al.,* 2009). After adsorption, the metal ions filled the pores in the activated carbon of ASAC and ZSAC. As well, the

particle size calculation was made by select 30 particles from SEM image and plotted against

frequency count and their distribution for particle size are given in Table 5.

Table 5   Particle size distribution of ASAC and ZSAC and Cu(II) and Cr(VI) ions– loaded ASAC and ZSAC

Sl.No.	Activated Carbon	Average Particle size (μm)
1	ASAC	2.76792 ± 0.06458
2	Cu(II) ion-loaded ASAC	4.14678 ± 0.15539
3	Cr(IV) ion-loaded ASAC	3 ± 0.05669
4	ZSAC	5.13147 ± 0.28423
5	Cu(II) ion-loaded ZSAC	6.29844 ± 0.17948
6	Cr(IV) ion-loaded ZSAC	3.09597 ± 0.37909

It could be illustrated that the prepared ASAC and ZSAC had s smaller size and is favourable for

Cu(II) ions and Cr(VI) ions adsorption (Jims *et al.,* 2018). After adsorption the size of the particle is

increases.

3.5.2 Energy Dispersive X-Ray Analysis

In order to confirm the adsorption of metal ion on to synthesized activated carbon EDS analysis was performed. During the EDX measurement *Allium sativm* activated carbon (ASAC), Cu(II) ion on ASAC, and Cr(VI) ion on ASAC, were focused and the corresponding peaks are shown in Fig. 9
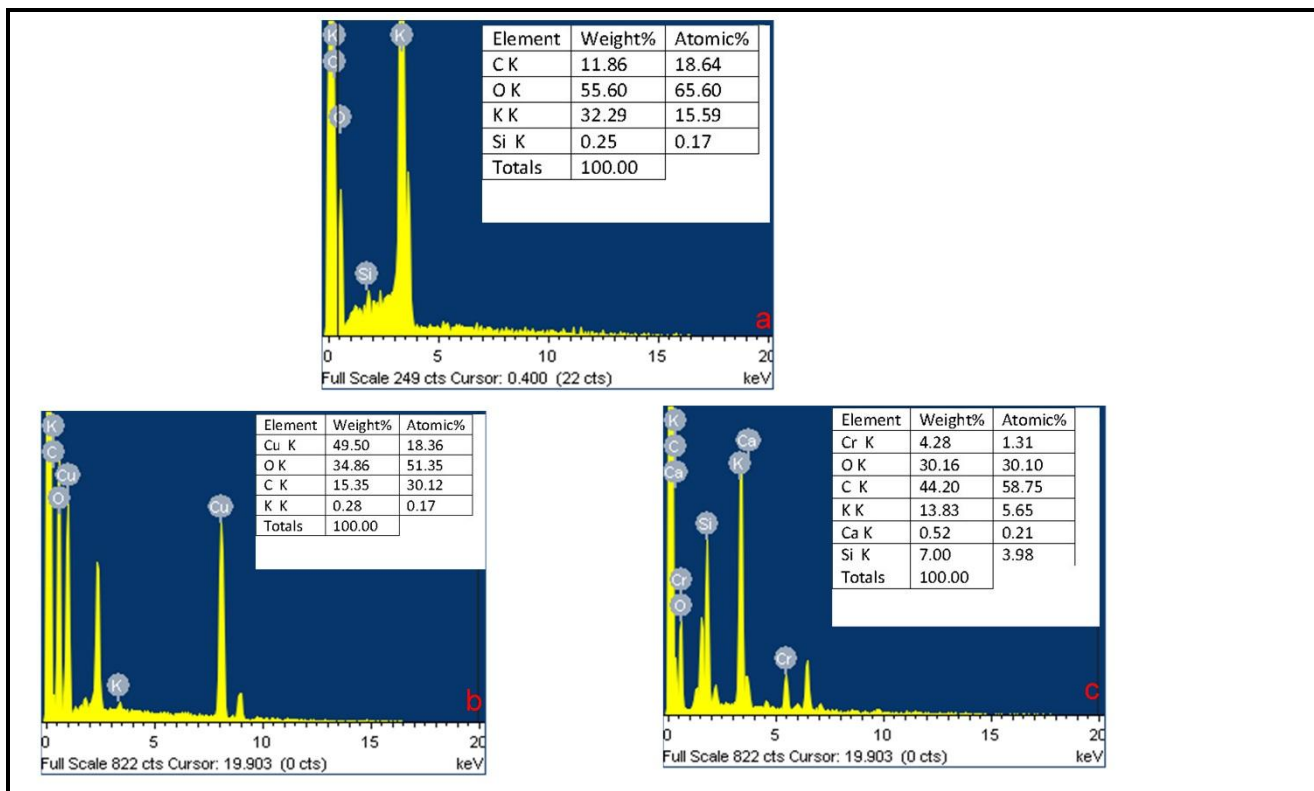
Fig. 9   Elemental analysis of (a) ASAC, (b) Cu(II) ion on ASAC and (c) Cr(VI) ion on ASAC

In ASAC, the quantity of Carbon, Oxygen, Potassium and Silicon were 18.64, 65.60, 15.59 and 0.17 respectively. While in Cu(II) ion adsorbed on ASAC, the values were 18.36, 51.35 and 30.12 measured in atomic percentage for copper, oxygen, and carbon respectively. While in Cr(VI) ion adsorbed on ASAC the values were 1.31, 58.75, 30.10, 5.65, 0.21 and 3.98 for Chromium, Carbon, Oxygen, Potassium, Calcium and Silicon respectively. Details of the EDX spectra values measured in atomic and weight % are listed in inside of the Table in Figure 9

Similarly, when focused ZSAC, Cu(II) ion on ZSAC and Cr(VI) ion on ZSAC EDX measurement gives corresponding peakes are shown in Figure 10.
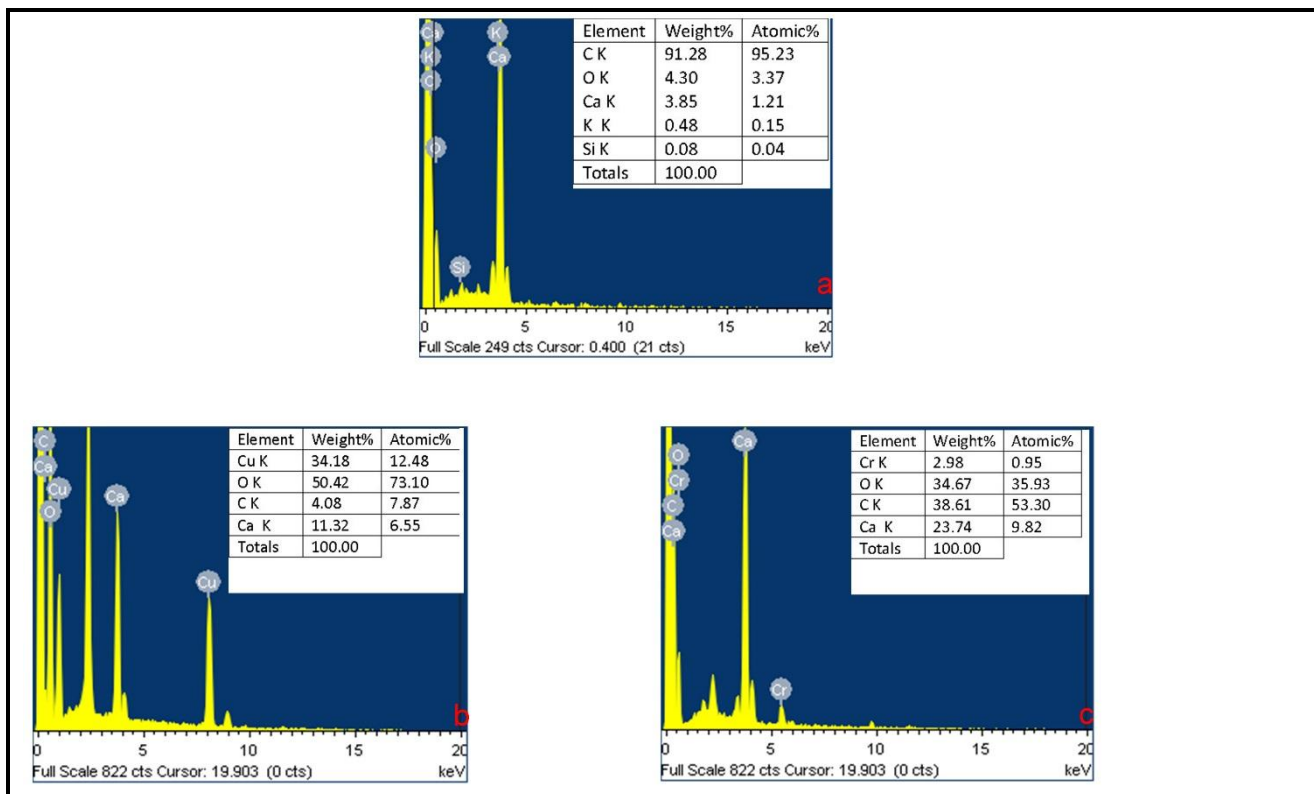
Fig. 10   Elemental analysis of (a) ZSAC, (b) Cu(II) ion on ZSAC and (c) Cr(VI) ion on ZSAC

In ZSAC, The quantity of Carbon, Oxygen, Calcium, Potassium and Silicon were 95.23, 3.37, 1.21, 0.15 and 0.04 respectively. While in Cu(II) ion adsorbed on ZSAC, the values were 12.48, 73.10, 7.87 and 6.55 measured in atomic percentage for Copper, Oxygen, Carbon and Calcium respectively. While in Cr(VI) ion adsorbed on ZSAC the values were 0.95, 35.93, 53.30 and 9.82 measured in atomic percentage for Chromium, Oxygen, Carbon and Calcium respectively. Details of the EDX Spectra values measured in atomic and weight % are listed in inside of the Table in Figure 10

In SEM_EDX analysis it can be surmised that the, prepared ASAC and ZSAC existing enough morphology for Cu(II) ion and Cr(VI) ion adsorption. (Jims *et al.,* 2018).

REFERENCES

Abdel-Nasser, A and Hendawy, EL 2006, 'Variation in the FTIR spectra of a biomass under impregnation carbonization and oxidation conditions', Journal of analytical and applied pyrolysis, vol.75, no.2, pp.159-166.

Abuzer, C and Huseyin, B 2011, 'Biosorption of cadmium and nickel ions using Spirulina Platensis: kinetic and equilibrium Studies', Desalination, vol. 275, no.1-3, pp.141-147.

Anah, I and Astrini, N 2017, 'Influence of pH on Cr(VI) ions removal from aqueous solutions using carbozymethyl cellulose – based hydrogel as adsorbent, IOP conf. series: Earth and Environmental Science 60.

Asep, BDN, Oktiani, R and Ragadhita, R 2019, 'How to read and interpret FTIR spectroscope of organic material', Indonesian Journal of science and Technology, vol.4, no.1, pp.97-118.

Azouaou, N, Sadaoui, Z, Djaafri, A and Mokaddem, H 2010 'Adsorption of cadmium from aqueous solution onto untreated coffee grounds: Equilibrium, kinetics and thermodynamics', Journal of Hazardous Materials, vol.184, pp. 126-134.

Bohli, T, Abdelmottaleb, O, Nuria, F and Isabel, V 2015, 'Evaluation of an activated Carbon from olive stones used as an adsorbent for heavy metal removal from aqueous phases', Competes Rendus Chimie, vol.18, no.1, pp. 88-99.

Chen, Y, Cao, X, Chang, PR and Huneault, MA, 2008, 'A comparative study on the films of poly (vinyl alcohol)/ pea starch nanocrystals and poly (vinyl alcohol)/ native pea starch', carbohydrate polymers, vol.73, no.1, pp.8-17.

Eren, E and Afsin, B 2008, 'An investigation of Cu(II) adsorption by raw and acid activated bentoniter : A combined potentiometric, thermodynamic, XRD, IR, DTA study', Journal of Hazardous Materials, vol. 151, no.2-3, pp. 682-691.

Fan, M, Dai, D and Huang, B 2012, 'Fourier transform infrared spectroscopy for natural fibres', In Fourier transform- materials analysis : In Tech.

Fierro V, and Celzard A 2007 'Studies in surface science and catalysis'.

Hariprasad Petal, Rajeshwari Sivaraj and Aniz Cu 2016, 'Preparation and characterization of activated carbon from Rice Husk, International Research Journal of Engineering and Technology, vol.3, no. 4, pp. 551-558.

Lumadede Mudoga, H 2002, 'A study on the use of activated carbon to remove colour in the sugar', https://www.researchgate.net/publication/264766625.

Ismail, A, Adie, DB, Oke, IA, Otun, JA, Olarinoye, NO, Lukman, S and Okuofu, CA 2009, 'Adsorption kinetics of cadmium ions onto powdered corn cobs', The Canadian Journal of Chemical Engineering, vol.87, no.6, pp.896-909.

Jims, JWG, Franklin, GA and Vijay, S 2018, 'Fabrication and Mechanical characterization of Stir Cast AA6063- Borosilicate fly ash Hybrid Metal Matrix Composites', International Journal o Sahira, J, Mandira, A, Bhadra, PP and Raja Ram, P 2013, 'Effects of activating agents on the activated carbons prepared from lapsi seed stone', Research Journal of Chemical Sciences, vol. 3.

Parmar, H, Jignesh, B, Patel, Padmaja Sudhakar and Koshy, VJ 2006, 'Removal of fluoride from water with powdered corn cobs', Journal of Environ, Science and Engg, vol. 48, no. 2, pp.135-138.

Sahira, J, Mandira, A, Bhadra, PP and Raja Ram, P 2013, 'Effects of activating agents on the activated carbons prepared from lapsi seed stone', Research Journal of Chemical Sciences, vol. 3.

Shahanaz Parvin and Biplob Kumar Biswas, 2021, 'Removal of congo Red by silver carp(Hypophthalmichthys molitrix) Fish Bone powder: kinetics, Equilibrium and thermodynamic study, Journal of chemistry, vol.2021.

Tongpoothorn, W, Somsimee, O, Somboon, T and Srittha, M 2019, 'An alternative and cost-effective biosorbent derived from napier grass stem for malachite green removal', Journal of materials and Environmental Sciences, vol.10, no.8, pp. 685-695.

Vunain, E, Kenneth, D and Biswick, T 2017, 'Synthesis and characterization of low- cost activated carbon prepared from Malawian baobab fruit shells by H_3PO_4 activation for removal of Cu(II) ions: equilibrium and kinetics studies', Applied water science, vol. 7, pp. 4301- 4319.